Accepted Manuscript

Novel pyrazolo[3,4-*d*]pyrimidine with 4-(1*H*-benzimidazol-2-yl)-phenylamine as broad spectrum anticancer agents: Synthesis, cell based assay, topoisomerase inhibition, DNA intercalation and bovine serum albumin studies

Prinka Singla, Vijay Luxami, Raja Singh, Vibha Tandon, Kamaldeep Paul

PII: S0223-5234(16)30856-X

DOI: 10.1016/j.ejmech.2016.09.093

Reference: EJMECH 8959

To appear in: *European Journal of Medicinal Chemistry*

Received Date: 13 May 2016

Revised Date: 3 September 2016

Accepted Date: 28 September 2016

Please cite this article as: P. Singla, V. Luxami, R. Singh, V. Tandon, K. Paul, Novel pyrazolo[3,4-*d*]pyrimidine with 4-(1*H*-benzimidazol-2-yl)-phenylamine as broad spectrum anticancer agents: Synthesis, cell based assay, topoisomerase inhibition, DNA intercalation and bovine serum albumin studies, *European Journal of Medicinal Chemistry* (2016), doi: 10.1016/j.ejmech.2016.09.093.

Graphical Abstract

Novel pyrazolo[3,4-*d*]pyrimidine with 4-(1*H*-benzimidazol-2-yl)-phenylamine as broad spectrum anticancer agents: Synthesis, cell based assay, topoisomerase inhibition, DNA intercalation and bovine serum albumin studies

Prinka Singla[1], Vijay Luxami[1]*, Raja Singh[2], Vibha Tandon[2] and Kamaldeep Paul[1]*

[1]*School of Chemistry and Biochemistry, Thapar University, Patiala – 147004, INDIA*

[2]*Special Centre for Molecular Medicine, Jawaharlal Nehru University, New Delhi-110 067, INDIA*

Email: kpaul@thapar.edu

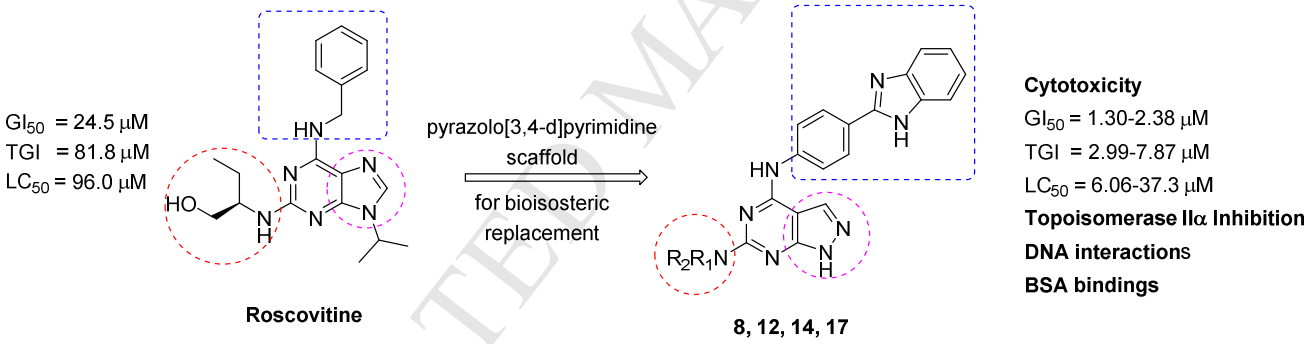

Novel pyrazolo[3,4-*d*]pyrimidine with 4-(1*H*-benzimidazol-2-yl)-phenylamine as broad spectrum anticancer agents: Synthesis, cell based assay, topoisomerase inhibition, DNA intercalation and bovine serum albumin studies

Prinka Singla[1], Vijay Luxami[1]* Raja Singh[2], Vibha Tandon[2], and Kamaldeep Paul[1]*

[1]*School of Chemistry and Biochemistry, Thapar University, Patiala – 147004, INDIA*

[2]*Special Centre for Molecular Medicine, Jawaharlal Nehru University, New Delhi-110 067, INDIA*

E-mail: kpaul@thapar.edu, vluxami@thapar.edu

Abstract: A series of new pyrazolo[3,4-*d*]pyrimidine possessing 4-(1*H*-benzimidazol-2-yl)-phenylamine moiety at C4 position and primary as well as secondary amines at C6 position has been designed and synthesized. Their antitumor activities were evaluated against a panel of 60 human cancer cell lines at National Cancer Institute (NCI). Six compounds displayed potent and broad spectrum anticancer activities at 10 μM. Compounds **8**, **12, 14** and **17** proved to be the most active and efficacious candidate in this series, with mean GI_{50} values of 1.30 μM, 1.43 μM, 2.38 μM and 2.18 μM, respectively against several cancer cell lines. Further biological evaluation of these compounds suggested that these compounds induce apoptosis and inhibit human topoisomerase (Topo) IIα as a possible intracellular target. UV-visible and fluorescence studies of these compounds revealed strong interaction with ct-DNA and bovine serum albumin (BSA).

Keywords: Pyrazolo[3,4-*d*]pyrimidine, Benzimidazole, Antitumor activity, ct-DNA, Bovine serum albumin.

1. Introduction

Cancer is a multifaceted disease that represents one of the leading causes of mortality, exceeded only by heart disease [1]. Although, chemotherapy is the main remedy for cancer treatment, but the use of available chemotherapeutics is often limited due to undesirable side effects and a limited choice of available anticancer drugs [2]. It is becoming important to investigate new agents and targets for the treatment of cancer. Thus, a considerable research for new anticancer agents has been fuelled by various industries and academics to unveil new targets and mechanisms based on the lead candidates of different classes of compounds [3].

Nitrogen heterocycles have received a great deal of attention in the literature due to their role as active pharmacophores. Roscovitine, belongs to the family of purine, is used for the treatment of non-

small cell lung cancer (NSCLC), leukemia, herpes simplex infection, Cushing's disease, HIV infection etc [4]. Roscovitine has been tested in several phase I and II clinical trials both as monotherapy and combination therapy in several human cancers. Roscovitine induces apoptosis in many cancer cell lines at all phases of the cell cycle [5]. In addition, roscovitine is also shown as synergistic effect with other anti-cancer agents, such as doxorubicin [6,7], taxol [7], 5-fluorouracil [7], vinblastine [7], alemtuzumab [8], paclitaxel [9], cisplatin [10], irinotecan [11], etoposide (cytotoxic anticancer drug, belongs to topoisomerase II enzyme inhibitor drug class [12] and tamoxifen [13]. Despite many successful preclinical studies with roscovitine, clinical trials are not very encouraging. Therefore, there is need for the contemporary medicinal chemists to further design and identify new potent purine analogue with improve anticancer activity [14].

Among the favorable bioisosteres to purine ring is pyrazolo[3,4-*d*]pyrimidine. Designing of pyrazolo [3,4-*d*]pyrimidine ring system has been taken to provide new compounds related with various biologically active purines, in the hope that new anti-tumor agents might be discovered. Literature survey revealed the interesting anticancer activities of certain pyrazolo[3,4-*d*]pyrimidine derivatives over various cancer cell lines [15]. Encouraging by the affirmative anticancer activity of several pyrazolo[3,4-*d*]pyrimidine members, and as a continuation of our ongoing efforts to identify new potent anticancer agents [16], a series of novel 6-substituted-2-benzimidazoanilino pyrazolo[3,4-*d*]pyrimidine has been synthesized. Our design is principally based on isosteric replacement of purine scaffold as well as installment of more lipophilic aromatic and aliphatic primary amines at C4 and C6 positions of pyrazolo[3,4-*d*]pyrimidine, respectively (Figure 1). We investigate the impact of replacing primary amines at C6 position with secondary amines on the antineoplastic activity. To the best of our knowledge, this substitution pattern of pyrazolo[3,4-*d*]pyrimidine is not explored so far, which motivated us to synthesize this type of compounds to explore their anticancer activity. Furthermore, the ability of these compounds to inhibit the relaxation activity of supercoiled pHOT1 DNA mediated by human topoisomerase IIα, suggest that nuclear enzyme is a potential intracellular target.

Figure 1

Since, it is commonly accepted that deoxyribonucleic acid (DNA) and proteins are considered as the main molecular targets in the action of drugs. Many compounds exert their drug effects through binding to DNA or proteins, which is the basis of designing and discovering new and more efficient drugs [17]. The studies on syntheses and interactions of small molecules with DNA and proteins have been an active field of research. The interaction of a small molecule with DNA initially causes

conformational changes in the double helix of DNA, subsequently interrupts replication, transcription, and repair, and finally kills the fast growing cells [18]. In the design of small molecules with DNA recognizing capacity, various pyrazolo[3,4-*d*]pyrimidine [19] have attracted much interest which damage DNA and cause cell death. Thus, pyrazolo[3,4-*d*]pyrimidine has attracted considerable attention owing to their capability of interacting with DNA.

Because of the high cost of using human serum albumin (HSA), bovine serum albumin (BSA) with lower cost is widely used as an important model protein concerning the interaction between compounds and serum albumins [20]. Compared with the number of organic molecules [21], relatively few pyrazolo[3,4-*d*]pyrimidine derivatives have been investigated for their protein, BSA-binding activity [22]. Therefore, the reactivity of pyrazolo[3,4-*d*]pyrimidine towards DNA and protein BSA is useful in the design and synthesis of anticancer therapeutics.

2. Results and Discussion

2.1. Chemistry

With a view to prepare the target [4-(1*H*-benzimidazol-2-yl)-phenyl]-(6-substituted-1*H*-pyrazolo[3,4-*d*]pyrimidin-4-yl)-amine, the key intermediate 4,6-dichloro-pyrazolo[3,4-*d*]pyrimidine (**4**) was synthesized from 5-aminopyrazole-4-carbonitrile **1**, which was prepared from 2-(ethoxymethylene) malononitrile. Condensation of commercially available 2-(ethoxymethylene)malononitrile with hydrazine afforded 5-aminopyrazole-4-carbonitrile (**1)** which underwent partial hydrolysis with sulphuric acid to produce 5-amino-1*H*-pyrazole-4-carboxamide (**2**) in good yield (89%). Treatment of carboxamide (**2**) with molten urea at 190 ^{0}C gave the intermediate product 1*H*-pyrazolo[3,4-*d*]pyrimidine-4,6(5*H*,7*H*)-dione (**3)**, that was easily chlorinated with excess phosphorous oxychloride, furnished 4,6-dichloropyrazolo[3,4-*d*]pyrimidine (**4**) in good yield (87%). As illustrated in Scheme 1, the substitution of 4-(1*H*-benzimidazol-2-yl)-phenylamine moiety (**5**) at C4 position of pyrazolo[3,4-*d*]pyrimidine was the next step for synthesis of the target compounds **7-18**. Nucleophilic displacement of 4,6-dichloropyrazolo[3,4-*d*]pyrimidine (**4**) with benzimidazole (**5**) was successfully accomplished under room temperature for 24 h in moderate yield (79%). ^{1}H NMR spectrum of **6**, showed the signals at δ 9.75 (s, 1H, ArH), 8.13-8.08 (m, 2H, ArH), 7.92 (d, 1H, ArH), 7.72 (d, 1H, ArH), 7.62 (bs, 1H, NH, D_2O exchangeable), 7.15-7.13 (m, 2H, ArH), 6.66 (d, 2H, ArH), 5.02 (bs, 1H, NH, D_2O exchangeable), while broad singlet of NH_2 protons at δ 4.45 of 4-(1*H*-benzimidazol-2-yl)-phenylamine disappeared in the ^{1}H NMR of compound **6**. The appendage of the second functionality, primary and secondary amines, at C6 position of pyrazolo[3,4-*d*]pyrimidine scaffold was achieved by refluxing of

amines in the presence of potassium carbonate in *n*-butanol, afforded the final compounds **7-18** (66-78%). The synthesized compounds were well characterized by NMR and mass spectrometry.

Scheme 1

2.2. In vitro evaluation for antitumor activity

The structure of the newly synthesized compounds were submitted to National Cancer Institute (NCI), Bethesda, Maryland, USA and six derivatives (**7, 8, 11, 12, 14** and **17**), were selected based on the degree of structural variation and computer modelling techniques for investigation of their anticancer activities. According to the NCI protocol, the selected compounds were first pre-screened at a single dose concentration of 10 μM towards the full panel of approximately 60 human cancer cell lines derived from 9 different cancer types: leukaemia, melanoma, lung, colon, central nervous system, ovarian, renal, prostate and breast cancers. The mean growth percentage (GP) for the full panel, as well as a range of GP with the lowest and the highest values among individual cancer cell lines are presented in Table 1.

As revealed from the results, all of the tested compounds, except **7** and **11**, displayed strong growth inhibitory activity (mean GP range of -77.92 to 57.44) over the examined cell lines at 10 μM concentration. The benzylamine derivative **14** demonstrated superior cytostatic activity while compound **12** (2-hydroxyethylpiperazine) showed better cytotoxic activities rather than pyrrolidine (**8**) and 4-fluororaniline (**17**). Such finding denotes that primary amine moiety is more favourable for cytostatic and secondary amine for cytotoxic anticancer activity. This superiority in the activity may be attributed to the corresponding increase in compound lipophilicity, and therefore permeability and penetration into cancer cells. By referring to the total number of sensitive cells for each tested compound, it was found that most of the target compounds exhibited broad spectrum antitumor activity covering different cancer cell lines. Among the responsive cell lines, U251 (CNS cancer) was noticed to be highly sensitive (minus GP values, lethal effect) for derivatives **11** and **12**. Melanoma cell lines SK-MEL-5 and LOX-IMVI were found to be the most susceptible cell lines for derivatives **14** and **17**, respectively. Moreover, the renal cancer cell line (786-0) was the most responsive cells to compound **8**. Compounds **8**, **12** and **14** showed pronounced cytotoxic activity over the majority of tested cell lines (> 50 cell lines), with mean GP values of -32.52, -77.92 and -8.30, respectively. Their detailed antiproliferative activities on the growth percentage of the NCI-60 cell lines, at single dose of 10 μM, are depicted in Figure S29-S34 (Supporting Information).

Table 1

Compounds **8**, **12**, **14** and **17** exhibited interesting growth inhibitory results in the preliminary single dose screen and were passed for the advanced 5-dose testing mode against the full panel. Three response parameters were calculated for each compound against each cell line: GI_{50} (the concentration producing 50% growth inhibition); TGI (the concentration leading to 100% growth inhibition); LC_{50} (the concentration causing 50% lethality). Moreover, the mean graph midpoint (MG-MID) were calculated for each of those parameters, producing an average activity parameter over all cell lines for the tested compounds. The subpanel and full panel MG-MID GI_{50} values of tested nine compounds along with roscovitine [23] as a reference compound are shown in Table 2.

Table 2

Investigation of the data listed in Table 2 clearly indicated remarkable potency of all compounds. All of the active compounds showed lower full panel MG-MID GI_{50} values (1.30-2.38 μM) than roscovitine (MG-MID GI_{50} value of 24.5 μM). Moreover, their subpanel MG-MID GI_{50} values over the majority of cancer types are better than those of the reference compound. The effect of substitution pattern of amine moiety at C6 position of pyrazolo[3,4-*d*]pyrimidine was examined. It has been observed that secondary amine derivatives **8** and **12** displayed superior antiproliferative potencies (MG-MID GI_{50} = 1.30 μM and 1.43 μM, respectively) rather the primary amine compounds **14** and **17** (MG-MID GI_{50} = 2.38 μM and 2.18 μM, respectively). Regarding the secondary amine, compound **8** with pyrrolidine moiety was slightly more potent than the corresponding 2-hydroxyethylpiperazine **12**. This may be owed to the differences in the electronic and/or steric effects of 2-hydroxyethylpiperazine in respect to pyrrolidine. Similarly, among the primary amine derivatives, compound **14** with benzyl amine showed reduced activity than 4-fluoroaniline member **17**. Therefore, it could be concluded that fluorine is preferential for achieving good antiproliferative activity. On the other hand, while considering the subpanel MG-MID GI_{50}, it was noticed that compounds **8** and **12** exhibited the best subpanel with GI_{50}, in most cases, are less than 2 μM. Since roscovitine is mainly active for non-small lung cancer (NSLC) and leukaemia, it is noteworthy mentioning that all compounds are highly potent than roscovitine over NSLC and leukaemia. In view of the efficacy relevant parameters (MG-MID TGI and MG-MID LC_{50} values) of the most potent compounds **8**, **12**, **14** and **17**, it was evident that all of them are highly effective than roscovitine. The pyrazolo[3,4-*d*]pyrimidines **8** and **12** exerted remarkable efficacies (MG-MID TGI < 5.00 μM and MG-MID LC_{50} < 11.0 μM) towards most of the

tested subpanel cancer cells. Interestingly, compounds **8** and **12** proved to be the most efficacious derivatives in this new series with full panel MG-MID TGI and LC_{50} values of 3.32 μM and 2.99 μM, and 10.5 μM and 6.06 μM, respectively (Figures S35-S46).

2.3. Topoisomerase IIα inhibitory activity

Based upon the antitumor activity, we investigated the ability of the active derivatives to inhibit relaxation activity catalysed by topoisomerase IIα. In these experiments, supercoiled plasmid DNA was incubated with Topo IIα at increasing concentrations of the compounds (10, 25, 50, 75, and 100 μM) and DNA relaxation products were then resolved by gel electrophoresis on 1% agarose gel. **Figure 2** showed the effect of the test compounds on the relaxation of supercoiled DNA mediated by topoisomerase IIα. Etoposide, a well-known DNA intercalating and DNA binding topoisomerase IIα inhibitor was used as a positive control at 25 μM concentration. In the presence of compounds **7**, **8**, **11**, **12**, **14** and **17**, the appearance of band corresponding to supercoiled DNA can be observed at 50 μM concentration, indicating inhibition of the topoisomerase IIα activity. Further investigation showed that these compounds also inhibit Topo IIα activity at both 75 μM and 100 μM concentrations. This data suggested that pyrazolo[3,4-*d*]pyrimidine compounds served as Topo IIα specific inhibitors at lower concentration. To check whether these compounds targets topoisomerase I enzyme, relaxation of supercoiled assay was performed, using camptothecin at 20 μM concentrations as positive control. As per our observations, these six compounds **7, 8, 11, 12, 14** and **17** did not show significant inhibition of Topo I activity even up to 100 μM concentration, suggesting that these pyrazolo[3,4-*d*]pyrimidine derivatives do not inhibit topoisomerase I.

Figure 2

2.4. DNA binding studies

UV-visible and fluorescence spectroscopy are frequently used techniques to studies the interactions between biological macromolecules and small molecules. We used UV-visible spectroscopy to investigate the absorbance spectra of compounds **7**, **8**, **11**, **12**, **14** and **17** with ct-DNA interaction in phosphate buffer (10 mM, pH 7.4) (Figure 3). The characteristic peaks of compounds were observed in the range of near 324-335 nm. However, on subsequent addition of ct-DNA to these compounds, the absorbance was gradually decreased, indicating hypochromic effect along with concomitant increase in absorption intensity at another λ_{max} = 257-264 nm (compound **7**; λ_{max} = 260 nm, compound **8**; λ_{max} = 259 nm, compound **11**; λ_{max} = 259 nm, compound **12**; λ_{max} = 259 nm, compound **14**; λ_{max} = 264 nm,

compound **17**; λ_{max} = 257 nm) (Table S1). Hypochromic effect of these compounds with ct-DNA indicates strong intermolecular interaction. This is due to the overlapping of electron cloud of pyrazolo[3,4-*d*]pyrimidine-benzimidazoles (compounds **7**, **8**, **11**, **12**, **14** and **17**) with ct-DNA base pairs [24]. Hypochromic effect in UV-visible spectra upon compounds, binding to ct-DNA is a characteristic of an intercalating binding mode [25].

Figure 3

Fluorescence experiments were also undertaken to investigate the interaction of synthesized compounds (**7**, **8**, **11**, **12**, **14** and **17**) with DNA. The binding of compounds with DNA, by maintaining the concentration of compounds constant (i.e., 10 μM), and varying the concentration of DNA from 0 to 20 μM, was studied by fluorescence spectroscopy. On excitation at 300 nm, these compounds showed intense band between 382 nm (compounds **7** and **14**) and 466 nm (compounds **8**, **11**, **12** and **17**). On increasing the concentration of ct-DNA to compounds, the fluorescence intensities were regularly decreasing while the maximum emission wavelength was slightly shifted in case of compounds **12** and **17** (Figure 4).

Figure 4

Subsequently, stabilities of pyrazolo[3,4-*d*]pyrimidine benzimidazoles–DNA complexes were determined by calculating the binding constant value from Benesi–Hildebrand equation [26].

$$1/(A_f - A_{obs}) = 1/(A_f - A_{fc}) + \{1/[K(A_f - A_{fc})]\}[\text{ligand}] \quad \text{------ 1}$$

where K is the binding constant, A_f is the absorbance of the free host, A_{obs} is the absorbance observed, and A_{fc} is the absorbance at saturation.

The plot of $1/(A_f - A_{obs})$ versus 1/[DNA] was constructed using the titration data and linear fitting, yielding the binding constant, in the order of 10^4 M^{-1} through absorption and emission titrations (Table S1). These calculated binding constant values showed moderate bindings of pyrazolo[3,4-*d*]pyrimidine-benzimidazoles with DNA. The results on stability agree with other DNA intercalating drugs, viz., 5-fluorouracil and mesalamine, which show 10^4 M^{-1} order of binding constant values [27]. This constant value might be sufficient to interfere with DNA replication and thus, could provide drug efficiency.

Further, ethidium bromide displacement studies have been performed with pyrazolo[3,4-*d*]pyrimidine-benzimidazoles for determination of binding mode. Ethidium bromide (EB) is one of the

sensitive fluorescent dye that binds to DNA via intercalative mode. In EB displacement assay, any molecule that binds to DNA via the same mode as EB will replace EB from the DNA helix and results in a decrease in the fluorescent intensity of EB.DNA system [28]. The EB.DNA complex showed the emission band at 606 nm. However, on subsequent addition of compounds **8**, **12**, **14** and **17** to the EB.DNA complex caused the decrease in emission band at 606 nm. There were significant changes in emission intensity of EB.DNA complex, suggesting that these compounds bind to DNA in intercalative mode (Figure S47).

2.5. Fluorescence quenching with bovine serum albumin (BSA).

Fluorescence quenching experiment is an efficient approach for exploring the binding mechanism of protein with ligand at molecular level [29]. The fluorescence measurements offer necessary information about the environment around fluorophore. Generally, the quenching process occurs due to a variety of molecular interactions viz., excited state reactions, molecular relocations, energy transfer, ground state complex development and collision [30]. Moreover, the binding of drug to BSA proteins may direct to loss or improvement of the biological properties of the original drug, or necessitate the paths for drug transportation [31]. Hence, the interaction of BSA with pyrazolo[3,4-*d*]pyrimidine-benzimidazole conjugates was studied by the fluorescence emission spectrum in the presence of different concentrations of compounds (0–30 μM). The emission spectra of BSA were recorded and the emission profile obtained at 298 K is represented in Figure 5. Bovine serum albumin demonstrates a strong fluorescence emission peak at ~352 nm on excitation at 280 nm. The result specifies that with increasing concentration of compounds **7**, **8**, **11**, **12**, **14** and **17**, the fluorescence intensity of BSA decreased regularly with an apparent quenching process. Moreover, upon the addition of these compounds, there were slightly λ_{em} blue shifts (4 nm at 20 μM pyrazolo[3,4-*d*]pyrimidine-benzimidazoles) of maximum emission wavelength, which signified non-covalent interactions via π–π stacking between the aromatic rings of compounds **7**, **8**, **11**, **12**, **14**, **17** and BSA with changes in protein conformation [32].

Figure 5

3. Conclusion

In summary, a series of new 6-substituted-pyrazolo[3,4-*d*]pyrimidine with 4-(1*H*-benzimidazol-2-yl)-phenylamine side chain at C4 position has been designed and synthesized as roscovitine analogues. A selected group of 6 compounds was assessed for its anticancer activity over a panel of 60 human cancer cell lines at 10 μM concentration. Most of the examined compounds, especially **8, 12, 14** and **17**

showed superior antitumor activities rather roscovitine over the majority of cancer cell lines with low micromolar GI_{50} values. A SAR study has been made and revealed the crucial role of both 4-(1*H*-benzimidazol-2-yl)-phenylamine and amines for attaining the best antineoplastic activity. Compound **8**, with pyrrolidine group, was noticed to be the most potent and efficacious member. Compounds **7**, **8**, **11, 12, 14** and **17** showed significant inhibition of human topoisomerase IIα relaxation activity at 50 μM concentration. To explore the possible binding capability of the newly synthesized analogs towards DNA, UV–vis and fluorescence techniques were used. Results from both studies predicted that pyrazolo[3,4-*d*]pyrimidine interacted with ct-DNA through intercalation mode. In the current study, the binding interaction of pyrazolo[3,4-*d*]pyrimidine with BSA has been studied by fluoresence spectroscopic method. It has been observed that pyrazolo[3,4-*d*]pyrimidine derivatives quench fluorescence of BSA with blue shift in maximum emission wavelength which signify the π-π interactions between the compounds and BSA. These findings are valuable in understanding the anticancer activity of this class of compounds as well as laying a foundation for the rational design of novel, powerful agents for probing and targeting nucleic acids and proteins, which are expected to provide an important insight into the field of DNA and protein interactions.

4. Experimental Section

4.1. Chemistry

All materials were obtained from commercial suppliers and used without further purification unless otherwise noted. Melting points were determined in open capillaries and were uncorrected. Reactions were monitored by thin-layer chromatography (TLC) carried out on silica gel plates (GF 254) using UV light as visualizing agent. Column chromatography was performed with silica gel mesh size 60-120. ^{1}H NMR and ^{13}C NMR spectra were recorded on Jeol-400 (^{1}H, 400 MHz; ^{13}C, 100 MHz) spectrometer at ambient temperature, using $CDCl_3$, and DMSO-d_6 as solvents. Chemical shifts are reported in parts per million (ppm) with TMS as an internal reference and *J* values are given in Hz. Mass spectrometric data were recorded at Waters Micromass Q-Tof Micro. Elemental analysis was done with Thermo Scientific (Flash 2000) analyzer. Hexane: ethylacetate and chloroform: methanol were the adopted solvent systems. UV-vis studies were carried out on a Specord PC machines using slit width of 1.0 nm and matched quartz cells. The fluorescence spectra were determined on a Varian Cary Eclipse fluorescence spectrometer.

*4.2. 5-Amino-1H-pyrazole-4-carbonitrile (**1**)*

Hydrazine (5 g, 0.156 mol) was carefully added into 2-(ethoxymethylene) malononitrile (8.64 g, 0.070 mol) in ethanol and heated on the steam-bath for 30 minutes. After completion of the reaction, white precipitate was gradually appeared that kept in a refrigerator overnight. The product was then filtered and washed with a small amount of cold ethanol to afford the desired product 5-amino-1*H*-pyrazole-4-carbonitrile (**1**) as white solid; (3.05 g, 86%); mp 168-170 ^{0}C (Lit. mp 169-170 ^{0}C) [33].

*4.3. 5-Amino-1H-pyrazole-4-carboxylic acid amide (**2**)*

5-Amino-1*H*-pyrazole-4-carbonitrile (**1**) (5g, 0.046 mol)) was added to cooled concentrated sulphuric acid (10 ml) with stirring so that the temperature did not rise above 20 ^{0}C. The addition took about one-half hour and solution was stirred at room temperature for 4 h. The acid solution was then poured with stirring into ice and the solution was kept overnight in the refrigerator. The solid was then filtered and washed with water to free of excess sulphuric acid to afford the desired product 5-amino-1*H*-pyrazole-4-carboxylic acid amide (**2**) as white solid; (5.19 g, 89%); mp 220-222 ^{0}C (Lit. mp 222-225 ^{0}C) [33].

*4.4. 1,7-Dihydro-pyrazolo[3,4-d]pyrimidine-4,6-dione (**3**)*

5-Amino-1*H*-pyrazole-4-carboxylic acid amide (**2**) **(**5g, 0.0396 mol) and urea (10 g, 0.1666 mol) were heated together at 190 ^{0}C for 20 minutes. The clear solution went mushy and heating was continued for another 20 minutes at 190 ^{0}C until the mushy melt became too solid to stir. The resulting solid was dissolved in hot dilute sodium hydroxide and the boiling basic solution was then carefully acidified with hydrochloric acid. The solution was allowed to stand approximately ten minutes and was then filtered to afford the desired product 1,7-dihydro-pyrazolo[3,4-*d*]pyrimidine-4,6-dione **(3)** as white solid; (3.73 g, 62%); mp > 300 ^{0}C [33].

*4.5. 4,6-Dichloro-1H-pyrazolo[3,4-d]pyrimidine (**4**)*

To 1,7-dihydro-pyrazolo[3,4-*d*]pyrimidine-4,6-dione **(3)** (1.233 mol), phosphorous oxychloride (2.84 mol) was added with stirring at 20 °C. After stirring for 15 min, the mixture was heated at 55 °C, and triethylamine (2.53 mol) was added over a period of 1 h at a rate that maintains the internal temperature below 65 °C, then mixture was slowly heated to an internal temperature of 85 °C for 10 min and then heated at 108-110 °C for 4 h to obtain a clear brown-yellow solution. The reaction mixture was cooled to an internal temperature of 40 °C and warm water was added over a period of

30-40 min. The solid was collected by filtration to afford pure 4,6-dichloro-1*H*-pyrazolo[3,4-*d*]pyrimidine (**4**) as light yellow solid; (5.35 g, 87 %); mp: 173-175 ^{o}C.

*4.6. 4-(1H-Benzimidazol-2-yl)-phenylamine (**5**)*

A mixture of 4-aminobenzoic acid (5 g, 5.78 mmol) and *o*-phenylenediamine (3.9 g, 3.68 mmol) were stirred in polyphosphoric acid (12.5 gm) at 200 ^{0}C for 5 h. The reaction mixture was cooled and poured into crushed ice. The precipitate was then stirred in cold water. Ammonium hydroxide solution was added until the pH 7 was achieved. The resulting solid was filtered and washed several times with methanol and column chromatographed on silica gel in ethylacetate: hexane (4:1) to afford the desired product 4-(1*H*-benzimidazol-2-yl)-phenylamine (**5**) as white solid; yield: 82%; mp: 207-209 ^{o}C; ^{1}H NMR (400 MHz, DMSO-d_6): δ = 7.96 (d, 2H, *J* = 8.72 Hz, ArH), 7.55-7.51 (m, 2H, ArH), 7.16-7.14 (m, 2H, ArH), 6.75 (d, 2H, *J* = 8.24 Hz, ArH), 4.45 (bs, 2H, NH_2); ^{13}C NMR (100 MHz, $CDCl_3$ + DMSO-d_6): δ = 152.2, 148.4, 127.5, 120.9, 118.6, 113.8 (ArC); MS (ESI), m/z: 210.2 (M^++1).

*4.7. [4-(1H-Benzimidazol-2-yl)-phenyl]-(6-chloro-1H-pyrazolo[3,4-d]pyrimidin-4-yl)-amine (**6**)*

To a solution of 4-(1*H*-benzimidazol-2-yl)-phenylamine (**5**) (1 g, 0.005 mol) in isopropyl alcohol (25 ml), 4,6-dichloro-1*H*-pyrazolo[3,4-*d*]pyrimidine (**4**) (0.99 g, 0.005 mol) was added and stirred at room temperature for 24 h. After washing the crude solid with isopropyl alcohol, dried to obtain pure [4-(1*H*-benzimidazol-2-yl)-phenyl]-(6-chloro-1*H*-pyrazolo[3,4-*d*]pyrimidin-4-yl)-amine (**6**) as white solid; yield: 79%; mp: > 300 ^{o}C; ^{1}H NMR (400 MHz, $CDCl_3$ + DMSO-d_6): δ = 9.75 (s, 1H, ArH), 8.13-8.08 (m, 2H, ArH), 7.92 (d, 1H, *J* = 8.60 Hz, ArH), 7.72 (d, 1H, *J* = 8.28 Hz, ArH), 7.62 (bs, 1H, NH), 7.15-7.13 (m, 2H, ArH), 6.66 (d, 2H, *J* = 8.72 Hz, ArH), 5.02 (s, 1H, NH); ^{13}C NMR (100 MHz, $CDCl_3$ + DMSO-d_6): δ = 147.6, 142.5, 132.2, 130.2, 129.3, 129.2, 124.0, 120.8 (ArC); MS (ESI), m/z: 362.7 (M^++1); Anal. Calcd for $C_{18}H_{12}ClN_7$: C, 59.76; H, 3.34; N, 27.10, Found: C, 59.83; H, 3.32; N, 27.14.

*4.8. General procedure for the preparation of compounds **7-18***

[4-(1*H*-Benzimidazol-2-yl)-phenyl]-(6-chloro-1*H*-pyrazolo[3,4-*d*]pyrimidin-4-yl)-amine **(6)** (0.100 g, 0.2 mmol) was refluxed with various amines (0.7 mol) in the presence of potassium carbonate (0.057 g, 0.4 mol) in *n*-butanol (20 ml) for 24 h and reaction was monitored by TLC; crude solid was obtained with evaporation of the solvent under vacuum that was purified by column chromatography using chloroform: methanol as eluents to give pure compounds **7-18**.

*4.8.1. [4-(1H-Benzimidazol-2-yl)-phenyl]-(6-morpholin-4-yl-1H-pyrazolo[3,4-d]pyrimidin-4-yl)-amine (**7**)*

White powder; yield: 77%; mp: > 300 ^{o}C; ^{1}H NMR (400 MHz, $CDCl_3$ + DMSO-d_6): δ = 8.08 (d, 2H, *J* = 8.72 Hz, ArH), 7.85 (s, 1H, ArH), 7.82 (d, 2H, *J* = 8.72 Hz, ArH), 7.76 (d, 2H, *J* = 8.68 Hz, ArH), 7.50 (bs, 1H, NH), 6.75 (d, 2H, *J* = 8.72 Hz, ArH), 3.86 (t, 6H, *J* = 5.04 Hz, mor-CH_2), 3.73-3.71 (m, 2H, mor-CH_2); ^{13}C NMR (100 MHz, $CDCl_3$ + DMSO-d_6): δ = 164.6, 163.8, 150.8, 142.6, 137.3, 127.1, 122.3, 120.8, 119.1, 114.1 (ArC), 66.0 (O-CH_2), 63.0 (N-CH_2); MS (ESI), m/z: 413.3 (M^++1); Anal. Calcd for $C_{22}H_{20}N_8O$: C, 64.07; H, 4.89; N, 27.17, Found: C, 64.45; H, 4.65; N, 27.45.

*4.8.2. [4-(1H-Benzimidazol-2-yl)-phenyl]-(6-pyrrolidin-1-yl-1H-pyrazolo[3,4-d]pyrimidin-4-yl)-amine (**8**)*

White powder; yield: 69%; mp: > 300 ^{o}C; ^{1}H NMR (400 MHz, $CDCl_3$ + DMSO-d_6): δ = 8.01 (d, 1H, *J* = 9.16 Hz, ArH), 7.98 (s, 1H, ArH), 7.88 (bs, 1H, NH), 7.86 (d, 1H, *J* = 8.68 Hz, ArH), 7.69 (d, 1H, *J* = 5.04 Hz, ArH), 7.67 (d, 1H, *J* = 5.04 Hz, ArH), 7.18 (d, 1H, *J* = 3.20 Hz, ArH), 7.17 (d, 1H, *J* = 3.20 Hz, ArH), 7.00 (t, 2H, *J* = 8.72 Hz, ArH), 3.61-3.59 (m, 4H, pyrr-CH_2), 1.99-1.94 (m, 4H, pyrr-CH_2); ^{13}C NMR (100 MHz, $CDCl_3$ + DMSO-d_6): δ = 163.9, 151.6, 138.7, 135.6, 135.2, 134.3, 133.2, 128.6, 127.5, 125.9, 122.7, 118.1, 116.4, 114.9, 114.7, 101.8 (ArC), 46.4 (N-CH_2), 29.2 (CH_2); MS (ESI), m/z: 397.4 (M^++1); Anal. Calcd for $C_{22}H_{20}N_8$: C, 66.65; H, 5.08; N, 28.26, Found: C, 66.51; H, 5.36; N, 28.31.

*4.8.3. [4-(1H-Benzimidazol-2-yl)-phenyl]-(6-piperidin-1-yl-1H-pyrazolo[3,4-d]pyrimidin-4-yl)-amine (**9**)*

White powder; yield: 72%; mp: > 300 ^{o}C; ^{1}H NMR (400 MHz, $CDCl_3$ + DMSO-d_6): δ = 8.46 (s, 1H, ArH), 8.31 (s, 1H, ArH), 8.12 (d, 1H, *J* = 8.72 Hz, ArH), 7.89 (d, 1H, *J* = 8.24 Hz, ArH), 7.70-7.66 (m, 1H, ArH), 7.61-7.59 (m, 2H, ArH), 7.22-7.19 (m, 1H, ArH), 7.03 (t, 1H, *J* = 8.24 Hz, ArH), 3.83-3.80 (m, 4H, pip-CH_2), 1.71-1.62 (m, 6H, pip-CH_2); ^{13}C NMR (100 MHz, $CDCl_3$ + DMSO-d_6): δ = 151.6, 142.2, 135.7, 135.5, 128.4, 127.3, 125.8, 120.8, 114.4, 114.2, 108.5 (ArC), 46.5 (N-CH_2), 26.2 (CH_2), 25.2 (CH_2); MS (ESI), m/z: 411.4 (M^++1); Anal. Calcd. for $C_{23}H_{22}N_8$: C, 67.30; H, 5.40; N, 27.30, Found: C, 67.07; H, 5.65; N, 27.18.

*4.8.4. [4-(1H-Benzimidazol-2-yl)-phenyl]-[6-(4-methyl-piperazin-1-yl)-1H-pyrazolo[3,4-d]pyrimidin-4-yl]-amine (**10**).*

White powder; yield: 74%; mp: > 300 ^{o}C; ^{1}H NMR (400 MHz, $CDCl_3$ + DMSO-d_6): δ = 8.14 (d, 1H, *J* = 8.68 Hz, ArH), 8.04 (s, 1H, ArH), 7.95 (bs, 1H, NH), 7.81 (d, 1H, *J* = 8.68 Hz, ArH), 7.64-7.60 (m,

2H, ArH), 7.22 (d, 1H, *J* = 3.20 Hz, ArH), 7.20 (d, 1H, *J* = 3.20 Hz, ArH), 7.04 (t, 2H, *J* = 8.68 Hz, ArH), 3.88 (t, 4H, *J* = 5.04 Hz, pip-CH_2), 2.53 (t, 2H, *J* = 4.56 Hz, pip-CH_2), 2.48 (t, 2H, *J* = 5.04 Hz, pip-CH_2), 2.30 (s, 3H, N-CH_3); ^{13}C NMR (100 MHz, $CDCl_3$ + DMSO-d_6): δ = 165.8, 158.5, 156.1, 151.6, 142.1, 135.6, 128.4, 127.3, 125.8, 114.4, 114.2, 108.5 (ArC), 46.5 (N-CH_2), 40.9 (N-CH_2), 13.4 (N-CH_3); MS (ESI), m/z: 426.5 (M^++1); Anal. Calcd for $C_{23}H_{23}N_9$: C, 64.92; H, 5.45; N, 29.63, Found: C, 64.74; H, 5.41; N, 29.75.

*4.8.5. N^6-(2-Amino-ethyl)-N^4-[4-(1H-benzimidazol-2-yl)-phenyl]-1H-pyrazolo[3,4-d]pyrimidine-4,6-diamine (**11**)*

White powder; yield: 73%; mp: > 300 °C; ^{1}H NMR (400 MHz, $CDCl_3$ + DMSO-d_6): δ = 8.12 (d, 1H, *J* = 8.68 Hz, ArH), 7.85 (bs, 1H, NH), 7.82-7.79 (m, 2H, ArH), 7.62-7.60 (m, 2H, ArH), 7.22-7.20 (m, 2H, ArH), 7.03 (t, 2H, *J* = 8.72 Hz, ArH), 3.64 (bs, 1H, NH), 3.53 (t, 2H, *J* = 4.12 Hz, N-CH_2), 2.99 (t, 2H, *J* = 5.52 Hz, N-CH_2); ^{13}C NMR (100 MHz, $CDCl_3$ + DMSO-d_6): δ = 148.7, 144.7, 135.1, 131.5, 128.3, 125.2, 119.5, 114.7, 114.5, 113.3 (ArC), 52.3 (N-CH_2), 42.6 (N-CH_2); MS (ESI), m/z: 386.1 (M^++1); Anal. Calcd for $C_{20}H_{19}N_9$: C, 62.32; H, 4.97; N, 32.71, Found: C, 62.45; H, 4.93; N, 32.65.

*4.8.6. 2-(4-{4-[4-(1H-Benzimidazol-2-yl)-phenylamino]-1H-pyrazolo[3,4-d]pyrimidin-6-yl}-piperazin-1-yl)-ethanol (**12**)*

White powder; yield: 72%; mp: > 300 °C; ^{1}H NMR (400 MHz, $CDCl_3$ + DMSO-d_6): δ = 8.14 (d, 1H, *J* = 9.16 Hz, ArH), 7.95 (s, 1H, ArH), 7.85 (bs, 1H, NH), 7.80 (d, 1H, *J* = 8.68 Hz, ArH), 7.63-7.59 (m, 3H, ArH), 7.23-7.19 (m, 2H, ArH), 7.04 (t, 1H, *J* = 8.92 Hz, ArH), 3.88 (t, 4H, *J* = 4.56 Hz, N-CH_2), 3.72 (t, 2H, *J* = 5.48 Hz, N-CH_2), 3.67 (t, 2H, *J* = 5.48 Hz, N-CH_2), 2.62-2.57 (m, 4H, N-CH_2); ^{13}C NMR (100 MHz, $CDCl_3$ + DMSO-d_6): δ = 164.4, 163.5, 163.1, 151.4, 142.2, 135.7, 134.8, 130.3, 128.3, 127.2, 125.8, 115.2, 109.2, 108.5 (ArC), 66.1 (O-CH_2), 46.4 (N-CH_2), 45.4 (N-CH_2), 43.0 (N-CH_2); MS (ESI), m/z: 456.1 (M^++1); Anal. Calcd for $C_{24}H_{25}N_9O$: C, 63.28; H, 5.53; N, 27.67, Found: C, 63.49; H, 5.49; N, 27.75.

*4.8.7.N^4-[4-(1H-Benzimidazol-2-yl)-phenyl]-N^6-(2-morpholin-4-yl-ethyl)-1H-pyrazolo[3,4-d]pyrimidine-4,6-diamine (**13**).*

White powder; yield: 70%; mp: > 300 °C; ^{1}H NMR (400 MHz, $CDCl_3$ + DMSO-d_6): δ = 8.43-8.23 (m, 1H, ArH), 8.10 (d, 2H, *J* = 8.68 Hz, ArH), 7.86 (s, 1H, NH), 7.66-7.58 (m, 3H, ArH), 7.20 (d, 1H, *J* = 3.20 Hz, ArH), 7.19 (d, 1H, *J* = 3.20 Hz, ArH), 7.04 (t, 1H, *J* = 8.24 Hz, ArH), 5.93 (bs, 1H, NH),

3.71-3.55 (m, 8H, mor-CH_2), 2.62 (t, 2H, *J* = 5.96 Hz, N-CH_2), 2.57-2.52 (m, 2H, N-CH_2); ^{13}C NMR (100 MHz, $CDCl_3$ + DMSO-d_6): δ = 165.3, 164.5, 163.7, 150.6, 137.2, 135.7, 135.1, 135.0, 128.4, 127.2, 125.3, 117.7, 114.8, 100.5 (ArC), 66.1 (O-CH_2), 52.9 (N-CH_2), 42.9 (N-CH_2), 36.5 (N-CH_2); MS (ESI), m/z: 456.1 (M^++1); Anal. Calcd for $C_{24}H_{25}N_9O$: C, 63.28; H, 5.53; N, 27.67, Found: C, 63.29; H, 5.49; N, 27.69.

4.8.8. N^4-[4-(1H-Benzimidazol-2-yl)-phenyl]-N^6-benzyl-1H-pyrazolo[3,4-d]pyrimidine-4,6-diamine ***(14)***

White powder; yield: 66%; mp: > 300 °C; ^{1}H NMR (400 MHz, $CDCl_3$ + DMSO-d_6): δ = 8.57 (bs, 1H, NH), 8.03 (d, 1H, *J* = 1.84 Hz, ArH), 7.32 (d, 1H, *J* = 8.72 Hz, ArH), 7.26 (d, 3H, *J* = 7.32 Hz, ArH), 7.21-7.16 (m, 3H, ArH), 7.13 (d, 3H, *J* = 8.72 Hz, ArH), 7.01 (d, 3H, *J* = 5.92 Hz, ArH), 5.27 (s, 2H, N-CH_2); ^{13}C NMR (100 MHz, $CDCl_3$ + DMSO-d_6): δ = 164.0, 163.8, 158.8, 156.4, 151.0, 137.9, 135.7, 135.3, 135.1, 134.2, 128.3, 127.2, 125.9, 121.8, 117.7, 116.1, 114.4, 114.2, 101.6 (ArC), 46.2 (N-CH_2); MS (ESI), m/z: 433.1 (M^++1); Anal. Calcd for $C_{25}H_{20}N_8$: C, 69.43; H, 4.66; N, 25.91, Found: C, 69.54; H, 4.62; N, 25.98.

4.8.9.2-{4-[4-(1H-Benzimidazol-2-yl)-phenylamino]-1H-pyrazolo[3,4-d]pyrimidin-6-ylamino}-ethanol ***(15)***

White powder; yield: 78%; mp: > 300 °C; ^{1}H NMR (400 MHz, $CDCl_3$ + DMSO-d_6): δ = 8.12 (t, 3H, *J* = Hz, ArH, NH), 8.02 (s, 1H, ArH), 7.80 (s, 2H, ArH), 7.63-7.61 (m, 1H, ArH), 7.50-7.45 (m, 1H, ArH), 7.19-7.16 (m, 1H, ArH), 7.00 (d, 1H, *J* = 7.32 Hz, ArH), 6.31 (bs, 1H, NH), 3.75 (t, 2H, *J* = 4.56 Hz, O-CH_2), 3.57 (t, 2H, *J* = 3.20 Hz, N-CH_2); ^{13}C NMR (100 MHz, $CDCl_3$ + DMSO-d_6): δ = 165.4, 163.6, 163.3, 151.3, 141.6, 135.1, 128.1, 127.0, 125.5, 121.0, 120.7, 114.1, 113.9, 108.2 (ArC), 60.5 (O-CH_2), 46.2 (N-CH_2); MS (ESI), m/z: 387.1 (M^++1); Anal. Calcd for $C_{20}H_{18}N_8O$: C, 62.17; H, 4.70; N, 29.00, Found: C, 62.24; H, 4.66; N, 29.20.

*4.8.10.N^6-Allyl-N^4-[4-(1H-benzimidazol-2-yl)-phenyl]-1H-pyrazolo[3,4-d]pyrimidine-4,6-diamine (**16**)*

White powder; yield: 69%; mp: > 300 °C; ^{1}H NMR (400 MHz, $CDCl_3$ + DMSO-d_6): δ = 8.13 (d, 1H, *J* = 8.68 Hz, ArH), 8.01 (d, 1H, *J* = 8.72 Hz, ArH), 7.76 (t, 1H, *J* = 8.72 Hz, ArH), 7.64-7.61 (m, 2H, ArH), 7.29-7.23 (m, 2H, ArH), 7.02 (d, 2H, *J* = 8.92 Hz, ArH), 6.62 (bs, 1H, NH), 6.02-5.93 (m, 1H, allyl-CH), 5.29 (d, 2H, *J* = 18.32 Hz, allyl-CH_2), 5.15 (d, 2H, *J* = 10.08 Hz, N-CH_2); ^{13}C NMR (100 MHz, $CDCl_3$ + DMSO-d_6): δ = 164.4, 150.5, 126.5, 121.8, 121.7, 119.2, 114.2, 114.0 (ArC), 53.9 (N-

CH_2); MS (ESI), m/z: 383.1 (M^++1); Anal. Calcd for $C_{21}H_{18}N_8$: C, 65.95; H, 4.74; N, 29.30, Found: C, 65.76; H, 4.71; N, 29.39.

*4.8.11. N^4-[4-(1H-Benzimidazol-2-yl)-phenyl]-N^6-(4-fluoro-phenyl)-1H-pyrazolo[3,4-d]pyrimidine-4,6-diamine (**17**)*

White powder; yield: 67%; mp: > 300 ^oC; ^1H NMR (400 MHz, $CDCl_3$ + DMSO-d_6): δ = 8.47 (bs, 1H, NH), 8.27 (s, 2H, ArH), 8.22 (d, 1H, *J* = 8.72 Hz, ArH), 7.92 (d, 1H, *J* = 8.68 Hz, ArH), 7.87 (d, 1H, *J* = 7.80 Hz, ArH), 7.69-7.66 (m, 4H, ArH), 7.29-7.27 (m, 1H, ArH), 7.09 (s, 1H, ArH), 7.05 (d, 2H, *J* = 8.68 Hz, ArH); ^{13}C NMR (100 MHz, DMSO-d_6): δ = 150.6, 139.8, 138.3, 138.1, 127.3, 124.4, 122.7, 122.5, 120.6, 120.5, 114.6, 114.8 (ArC); MS (ESI), m/z: 437.1 (M^++1); Anal. Calcd for $C_{24}H_{17}FN_8$: C, 66.05; H, 3.93; N, 25.67, Found: C, 66.41; H, 3.89; N, 25.61.

*4.8.12. N^4-[4-(1H-Benzimidazol-2-yl)-phenyl]-N^6-cyclohexyl-1H-pyrazolo[3,4-d]pyrimidine-4,6-diamine (**18**)*

White powder; yield: 68%; mp: > 300 ^oC; ^1H NMR (400 MHz, $CDCl_3$ + DMSO-d_6): δ = 8.27 (bs, 1H, NH), 8.16 (s, 1H, ArH), 8.11 (d, 1H, *J* = 8.72 Hz, ArH), 7.90 (d, 1H, *J* = 6.88 Hz, ArH), 7.84 (s, 1H, ArH), 7.68-7.65 (m, 3H, ArH), 7.20-7.17 (m, 1H, ArH), 7.01 (t, 1H, *J* = 8.68 Hz, ArH), 5.54 (bs, 1H, NH), 3.87-3.84 (m, 1H, CH), 2.06-2.04 (m, 2H, CH_2), 1.86-1.60 (m, 4H, CH_2), 1.39-1.08 (m, 4H, CH_2); ^{13}C NMR (100 MHz, $CDCl_3$ + DMSO-d_6): δ = 151.6, 142.2, 135.3, 133.8, 130.8, 128.3, 127.2, 125.6, 115.7, 110.2, 108.5 (ArC), 52.8 (N-CH_2), 46.5 (CH_2), 43.0 (CH_2), 36.4 (CH_2); MS (ESI), m/z: 425.2 (M^++1); Anal. Calcd for $C_{24}H_{24}N_8$: C, 67.90; H, 5.70; N, 26.40, Found: C, 67.72; H, 5.50; N, 26.21.

4.9. Procedure for in vitro anticancer screening

The human tumor cell lines of cancer screening were grown in RPMI 1640 medium containing 5% fetal bovine serum and 2 mM L-glutamine. Cells were inoculated in 96 well plates in 100 μL per well at plating densities ranging from 5,000 to 40,000 cells/well that depends upon the doubling time of individual cell lines. The microtiter plates were then incubated at 37 $^\circ C$, 95% air, 5% CO_2, and 100% relative humidity for 24 h. Two plates of each cell line were then fixed *in situ* with TCA. Experimental drugs were dissolved in DMSO at 400-fold the desired final maximum test concentration and stored frozen prior to use. At the time of drug addition, an aliquot of frozen concentrate was used and diluted to two times the desired final maximum test concentration with complete medium containing 50 μg/ml gentamicin. Additional four, 10-fold or ½ log serial dilutions were made to give total of five drug

concentrations plus control. Aliquots of 100 μL of these drug dilutions were added to the appropriate microtiter wells. Following the addition, plates were incubated at 37 $^{\circ}$C, 5% CO_2, 95% air, and 100% relative humidity for 48 h. For adherent cells, the assay was terminated by the addition of cold TCA. Cells were fixed *in situ* by the addition of 50 μL of cold 50% (w/v) TCA and incubated at 4 $^{\circ}$C for 60 min. The plates were washed five times with tap water by discarding the supernatant and air dried. Sulphorhodamine B (SRB) solution (100 µL) at 0.4% (w/v) in 1% acetic acid was added to each well followed by incubation of plates for 10 min at room temperature. After staining, unbound dye was removed by washing five times with 1% acetic acid and the plates were air dried before subsequent solubilization with 10 mM trizma base. The absorbance was read at a wavelength of 515 nm on an automated plate reader. With seven absorbance measurements [time zero (T_z), control growth (C), and test growth in the presence of drug at five concentration levels (T_i)], percentage growth was calculated at each of the drug concentration levels. Percentage growth inhibition was calculated as:

[(Ti -Tz)/(C - Tz)] × 100 for concentrations for which $T_i \geq Tz$; [(Ti -Tz)/Tz] × 100 for concentrations for which Ti < Tz.

Three dose response parameters were calculated for each experimental agent. Growth inhibition of 50% (GI_{50}) was calculated from [(Ti -Tz)/(C - Tz)] × 100 = 50. Drug concentration resulting in total growth inhibition (TGI) was calculated from T_i = Tz. LC_{50} was calculated from [(Ti-Tz)/Tz]×100 = 50.

4.10. Relaxation Assay of Human Topoisomerase IIα.

Relaxation of negatively supercoiled plasmid DNA by human topoisomerase IIα was assayed in 20 μL of reaction buffer (50 mM Tris-Cl, pH 8.0, 120 mM KCl, 10 mM $MgCl_2$, 0.5 mM ATP, 0.5 mM dithiothreitol) containing 500 ng of supercoiled pHOT1 plasmid DNA and 1 unit of Topo IIα enzyme. After incubation at 37 °C for 30 min, the reactions were stopped by the addition of 5 ml of 50% glycerol, 50 mM EDTA, and 0.5% (v/v) bromophenol blue. After electrophoresis in 1 % agarose gel with 1XTBE buffer (1 litre of 5X stock solution-54 g of tris base, 27.5 g of boric acid, 20 ml of 0.5 M EDTA pH 8.1), the DNA was stained with ethidium bromide and photographed over UV light.

4.11. Procedure for DNA binding studies

4.11.1. Materials and methods

The stock solution of ct-DNA (Sigma Chemical Co., USA) was prepared by dissolving an appropriate amount of ct-DNA in Millipore water. The purity of ct-DNA was verified by monitoring the ratio of

the absorbance at 260 and 280 nm, and the ratio of A_{260}/A_{280} was 1.82, indicating that ct-DNA was sufficiently free of protein contamination. The concentration of ct-DNA in terms of the nucleotide phosphate (i.e. nucleotide) was determined to be 2.56×10^{-3} $molL^{-1}$ by UV-vis absorption at 260 nm using a molar absorption coefficient of $\varepsilon_{260} = 6600$ L $mol^{-1}cm^{-1}$(expressed as the molarity of phosphate groups). All stock solutions were diluted to the required concentrations with phosphate buffer (pH 7.4). All other reagents were of analytical reagent grade, and ultrapure water was used throughout the experiment. All stock solutions were stored at 0–4 ^{0}C.

4.11.2. UV-vis absorption spectra

All the spectra were recorded at ambient temperature (300 K). UV-vis spectra were recorded on Shimadzu-2400 PC spectrometer with 1 cm cuvette. Any background buffer signal was electronically subtracted. Absorption titrations were performed with constant ligand concentration of 20 μM and increasing ct-DNA concentration (up to 15 μM). The control experiment was done by adding equal volumes of buffer solution instead of DNA solution to the same concentration of compound. The control experiment shows no significant change in the absorption spectra of the compound.

4.11.3. Fluorescence spectra

Emission spectra were recorded with Varian Cary Eclipse fluorescence spectrometer. Fluorescence titration spectra were obtained with a constant ligand concentration (20 μM) and increasing amount of ct-DNA (up to 17 μM).

4.11.4. Binding constants

Binding constant K for the ligand–DNA complex was estimated from absorption and fluorescence titration data using the Benesi–Hildebrand equation-1 that suggested strong interactions with ct-DNA.

$$1/(A_f - A_{obs}) = 1/(A_f - A_{fc}) + \{1/[K(A_f - A_{fc})]\}[\text{ligand}] \quad \text{------ 1}$$

where K is the binding constant, A_f is the absorbance of the free host, A_{obs} is the absorbance observed, and A_{fc} is the absorbance at saturation.

K was determined from the ratio of intercept to slope obtained from the linear fit of the plot of $1/(A_f - A_{obs})$ versus 1/[DNA], respectively. The control experiment was done by adding equal volumes of buffer solution instead of DNA solution to the same concentration of the compound. No significant change in the emission spectra was observed in control experiment.

4.11.5. Competitive binding study of compounds with ct-DNA in the presence of ethidium bromide

Competitive binding of compounds with DNA in the presence of intercalator ethidium bromide were studied. Ethidium bromide was dissolved in Milli-Q water to prepare a stock solution with 1 mM strength and diluted immediately before use. Fluorescence spectra were taken in the presence of ethidium bromide while increasing the amount of ct-DNA (0 to 20 μM) and using an excitation wavelength of 480 nm. Compounds were added with increasing concentration of 2 μM (up to 50 μM), mixed thoroughly after each addition and the emission spectrum was recorded with λ_{ex} = 480 nm.

4.12. Procedure for BSA screening

4.12.1. Materials and methods

The stock solution of BSA (Sigma Chemical Co., USA) was prepared by dissolving an appropriate amount of solid BSA in 0.1 M phosphate buffer at pH 7.4 and stored at 0−4 °C in the dark. Stock solutions of compounds **7-18** (10^{-3} mol L^{-1}) were prepared in DMSO. All stock solutions were diluted to the required concentrations with phosphate buffer (pH 7.4). All other reagents were of analytical reagent grade.

4.12.2. Fluorescence spectra

Emission spectra were recorded with Varian Cary Eclipse fluorescence spectrometer. The excitation and emission wavelengths for BSA were 280 nm and 351 nm with a slit width of 10 nm. Very dilute solutions of BSA and compounds **7-18** were used to avoid inner filter effect. The titration experiments were performed by varying the concentration of compounds **7-18** and keeping the BSA concentration (10 μM).

ACKNOWLEDGMENTS

KP thanks the Department of Science and Technology, New Delhi (EMR/2014/000669). PS is grateful for a DST/Inspire Fellowship (Fellow Code-IF110542). NIH, Bethesda, USA for anticancer activities and SAI labs, Thapar University are also acknowledged.

REFERENCES

[1] A. Jemal, R. Siegel, E. Ward, T. Murray, J. Xu, M.J. Thun, Cancer Statistics 2007. Cancer J.

Clin. 57 (2007) 43-66.

[2] (a) J.B. Gibbs, Mechanism-based target identification and drug discovery in cancer research. Science 287 (2000) 1969-1971. (b) C. Unger, New therapeutic approaches in cancer treatment. Drug Future 22 (1997) 1337-1345.

[3] J.E. Dancey, H.X. Chen, Strategies for optimizing combinations of molecularly targeted anticancer agents. Nat. Rev. Drug Discov. 5 (2006) 649-659.

[4] W.F. De Azevedo, S. Leclerc, L. Meijer, L. Havlicek, M. Strnad, S.-H. Kim, Inhibition of cyclin-dependent kinases by purine analogues: crystal structure of human cdk2 complexed with roscovitine. Eur. J. Biochem. 243 (1997) 518-526.

[5] S.J. McClue, D. Blake, R. Clarke, A. Cowan, L. Cummings, P.M. Fischer, M. MacKenzie, J. Melville, K. Stewart, S. Wang, N. Zhelev, D. Zheleva, D. P. Lane, In vitro and in vivo antitumor properties of the cyclin dependent kinase inhibitor CYC202 (R-roscovitine). Int. J. Cancer 2002, 102, 463-468.

[6] L.A. Lambert, N. Qiao, K.K. Hunt, D.H. Lambert, G.B. Mills, L. Meijer, K. Keyomarsi, Autophagy: a novel mechanism of synergistic cytotoxicity between doxorubicin and roscovitine in a sarcoma model. Cancer Res., 68 (2008) 7966-7974.

[7] M.S. Abaza, A.M. Bahman, R.J. Al-Attiyah, Roscovitine synergizes with conventional chemo-therapeutic drugs to induce efficient apoptosis of human colorectal cancer cells. World J. Gastroenterol., 14 (2008) 5162-5175.

[8] E. Weingrill, A. Wölfler, D. Strunk, W. Linkesch, H. Sill, P.M. Liebmann, Roscovitine in B-chronic lymphocytic leukemia cells: High apoptosis-inducing efficacy and synergism with alemtuzumab independent of the patients' pretreatment status. Haematologica 92 (2007) 1286-1288.

[9] H.M. Coley, C.F. Shotton, H. Thomas, Seliciclib (CYC202; r-roscovitine) in combination with cytotoxic agents in human uterine sarcoma cell lines. Anticancer Res., 27 (2007) 273-278.

[10] H.M. Coley, C.F. Shotton, M.I. Kokkinos, H. Thomas, The effects of the CDK inhibitor seliciclib alone or in combination with cisplatin in human uterine sarcoma cell lines. Gynecol. Oncol., 105 (2007) 462-469.

[11] M. Abal, R. Bras-Goncalves, J.G. Judde, H. Fsihi, P De Cremoux, D. Louvard, H. Magdelenat, S. Robine, M.F. Poupon, Enhanced sensitivity to irinotecan by Cdk1 inhibition in the p53-deficient HT29 human colon cancer cell line. Oncogene, 23 (2004) 1737-1744.

[12] S.L. Maude, G.H. Enders, Cdk inhibition in human cells compromises Chk1 function and

activates a DNA damage response. Cancer Res., 65 (2005) 780-786.

[13] D. Gritsch, M. Maurer, N. Zulehner, J. Wesierska-Gadek, Tamoxifen enhances the anti-proliferative effect of roscovitine, a selective cyclin-dependent kinase inhibitor, on human ER-positive human breast cancer cells. J. Exp. Ther. Oncol., 9 (2011) 37-45.

[14] J. Cicenas, K. Kalyan, A. Sorokinas, E.Stankunas, J. Levy, I. Meskinyte, V. Stankevicius, A. Kaupinis, M. Valius, Roscovitine in cancer and other diseases. Ann. Transl. Med. 3 (2015) 135.

[15] (a) M. Chauhan, R. Kumar, Medicinal attributes of pyrazolo[3,4-d]pyrimidines: A review, Bioorg. Med. Chem. 21 (2013) 5657–5668; (b) J.M. Quintelaa, C. Peinadora, M.J. Moreiraa, A. Alfonsob, L.M. Botanab, R. Riguerac, Pyrazolopyrimidines: synthesis, effect on histamine release from rat peritoneal mast cells and cytotoxic activity, Eur. J. Med. Chem. 36 (2001) 321–332. (c) N.S.M. Ismail, E.M.H. Ali, D.A. Ibrahim, R.A.T. Serya, D.A. Abou El Ella, Pyrazolo[3,4-*d*]pyrimidine based scaffold derivatives targeting kinases as anticancer agents, Future J. Pharm. Sci. 2016, doi:10.1016/j.fjps.2016.02.002

[16] (a) A. Sharma, V. Luxami, K. Paul, Purine-benzimidazole hybrids: synthesis, single crystal determination and in vitro evaluation of antitumor activities. Eur. J. Med. Chem. 93 (2015) 414-422; (b) P. Singla, V. Luxami, K. Paul, Synthesis and in vitro evaluation of novel triazine analogues as anticancer agents and their interaction studies with bovine serum albumin, Eur. J. Med. Chem. 117 (2016) 59-69; (c) Richa Goel, V. Luxami, K. Paul, Synthesis, in vitro anticancer activity and SAR studies of arylated imidazo[1,2-a]pyrazine-coumarin hybrids, RSC Adv. 5 (2015) 37887-37895.

[17] (a) E. Meggers, From conventional to unsual enzyme inhibitor scaffolds: The quest for target specificity. Angew. Chem., Int. Ed., 50 (2011) 2442–2448; (b) G. Sava, G. Jaouen, E.A. Hillard, A. Bergamo, Targeted therapy *vs.* DNA-adduct formation-guided design: thoughts about the future of metal-based anticancer drugs. Dalton Trans., 41 (2012) 8226–8234; (c) C.G. Hartinger, N. Metzler-Nolte, P.J. Dyson, Challenges and opportunity in the development of organometallic anticancer drugs. Organometallics, 31 (2012) 5677–5685; (d) N.P.E. Barry, P.J. Sadler, Exploration of the medical periodic table: towards new targets. Chem. Commun., 49 (2013) 5106–5131.

[18] (a) G. Momekov, A. Bakalova, M. Karavanova, Novel approaches towards development of non-classical platinum-based antineoplastic agents: design of platinum complexes characterized by an alternative DNA-binding pattern and/or tumor-targeted cytotoxicity, Curr. Med. Chem. 12 (2005) 2177-2191; (b) L.H. Hurley, DNA and its associated processes as targets for cancer

therapy, Nat. Rev. Cancer 2 (2002) 188-200; (c) R. Martinez, L. Chacon-Garcia, The search for DNA-intercalators as antitumoral drugs; what worked and what did not work, Curr. Med. Chem. 12 (2005) 127-151.

[19] (a) E.R. el-Bendary, F.A. Badria. Synthesis, DNA-binding, and antiviral activity of certain pyrazolo[3,4-d]pyrimidine derivatives. Arch Pharm (Weinheim). 333 (2000) 99-103; (b) A. Spreafico, S. Schenone, T. Serchi, M. Orlandini, A. Angelucci, D. Magrini, G. Bernardini, G. Collodel, A. Di Stefano, C. Tintori, M. Bologna, F. Manetti, M. Botta, A. Santucci, Antiproliferative and proapoptotic activities of new pyrazolo[3,4-*d*]pyrimidine derivative Src kinase inhibitors in human osteosarcoma cells, The FASEB Journal 22 (2008) 1560-1571; (c) A.T. Baviskar, U.C. Banerjee, M. Gupta, R. Singh, S. Kumar, M.K. Gupta, S. Kumar, S.K. Raut, M. Khullar, S. Singh, R. Kumar, Synthesis of imine-pyrazolopyrimidinones and their mechanistic interventions on anticancer activity Bioorg. Med. Chem. 21 (2013) 5782–5793.

[20] H. Benyamini, A. Shulman-Peleg, H.J. Wolfson, B. Belgorodsky, L. Fadeev, M. Gozin, Interaction of C_{60}-fullerene and carboxyfullerene with proteins: Docking and binding site alignment, Bioconjugate Chem., 17 (2006) 378–386.

[21] (a) D. Lu, X. Zhao, Y. Zhao, B. Zhang, B. Zhang, M. Geng, R. Liu, Binding of Sudan II and Sudan IV to bovine serum albumin: Comparison studies, Food Chem. Toxicol., 49 (2011) 3158–3164; (b) P. Bolel, N. Mahapatra, S. Datta, M. Halder, Modulation of accessibility of subdomain IB in the pH-dependent interaction of bovine serum albumin with cochineal red A: A combined view from spectroscopy and docking simulations, J. Agric. Food Chem., 61 (2013) 4606–4613.

[22] G. Vignaroli, P. Calandro, C. Zamperini, F. Coniglio, G. Iovenitti, M. Tavanti, D. Colecchia, E. Dreassi, M. Valoti, S. Schenone, M. Chiariello, M. Botta, Improvement of pyrazolo[3,4-*d*]pyrimidines pharmacokinetic properties: nanosystem approaches for drug delivery, Sci. Rep. 6 (2016) 21509. (b) T. Gabriel, Y. Lou, P38 MAP kinase inhibitors and methods for using the same, US 20080146590 (2008); (c) K.R. Woller, M.L. Curtin, K.E. Frank, N.S. Josephsohn, B.C. Li, N. Wishart, Novel pyrazolo[3,4-*d*]pyrimidine compounds, US 20120015963 (2012).

[23] Anticancer activity of roscovitine available in NCI data base (www.dtp.nci.nih.gov), NSC 701554.

[24] (a) R. Fukuda, S. Takenaka, M. Takagi, Metal ion assisted DNA-intercalation of crown ether-linked acridine derivatives, J. Chem. Soc. Chem. Commun. 1 (1990) 1028-1030. (b) J. Kapuscinski, Z. Darzynkiewicz, Interactions of antitumor agents ametantrone, and mitoxantrone (novatrone) with double-stranded DNA, Biochem. Pharmacol. 34 (1985) 4203-4213.

[25] N. Li, Y. Ma, C. Yang, L. Guo, X. Yang, Interaction of anticancer drug mitoxantrone with DNA analyzed by electrochemical and spectroscopic methods, Biophys. Chem. 116 (2005) 199-205.

[26] H.A. Benesi, J.H. Hildebrand, A spectrophotometric investigation of the interaction of iodine with aromatic hydrocarbons, J. Am. Chem. Soc., 71 (1949) 2703-2707.

[27] (a) N. Shahabadi, S.M. Fili, F. Kheirdoosh, Study on the interaction of the drug mesalamine with calf thymus DNA using molecular docking and spectroscopic techniques, J. Photochem. Photobiol. B 128 (2013) 20-26; (b) R. Palchaudhuri, P.J. Hergenrother, DNA as a target for anticancer compounds: methods to determine the mode of binding and the mechanism of action, Curr. Opin. Biotechnol. 18 (2007) 497-503.

[28] John Olmsted III, David R. Kearns, Mechanism of ethidium bromide fluorescence enhancement on binding to nucleic acids, Biochemistry 16 (1977) 3647–3654

[29] J. Shi, J. Wang, Y. Zhu, J. Chen, Characterization of interaction between isoliquiritigenin and bovine serum albumin: Spectroscopic and molecular docking methods, J. Lumin., 145 (2014) 643–650.

[30] I.P. Caruso, W. Vilegas, M.A. Fossey, M.L. Cornelio, Exploring the binding mechanism of Guaijaverin to human serum albumin: Fluorescence spectroscopy and computational approach, Spectrochim. Acta A Mol. Biomol. Spectrosc. 97 (2012) 449–455

[31] C. Tan, J. Liu, H. Li, W. Zheng, S. Shi, L. Chen, L. Ji, Differences in structure, physiological stability, electrochemistry, cytotoxicity, DNA and protein binding properties between two Ru(III) complexes, J. Inorg. Biochem. 102 (2008) 347–358.

[32] V. Rajendiran, R. Karthik, M. Palaniandavar, H. Stoeckli-Evans, V.S. Periasamy, M.A. Akbarsha, B.S. Srinag, H. Krishnamurthy, Mixed-Ligand Copper(II)-phenolate Complexes: Effect of Coligand on Enhanced DNA and Protein Binding, DNA Cleavage, and Anticancer Activity, Inorg. Chem. 46 (2007) 8208–8221.

[33] R.K. Robins, Potential purine antagonists. I. Synthesis of some 4,6-substituted pyrazolo [3,4-*d*] pyrimidines, J. Am. Chem. Soc., 78 (1956) 784-790.

Figures Captions

Figure 1. Rational design of the target compounds

Figure 2. Inhibition of relaxation activity of Topo IIα in the presence of compounds **7, 8**, **11, 12, 14** and **17**. Ethidium bromide stained agarose gel showing: lane 1, pHOT1 plasmid DNA (C); lane 2, relaxation of plasmid DNA by Topo IIα (EC); lanes 3–7 for compound **7** (**A**), lanes 8-12 for compound **8** (**A**) and lanes 13-17 for compound **11** (**A**); lanes 3–7 for compound **12** (**B**), lanes 8-12 for compound **14** (**B**) and lanes 13-17 for compound **17** (**B**) inhibition of relaxation of plasmid DNA by Topo IIα in the presence of 10, 25, 50, 75 and 100 μM of compounds, respectively. Lane 18 indicated the etoposide at 25 μM as positive control (PC).

Figure 3. UV-Vis spectral changes of compounds **7, 8, 11, 12, 14** and **17** at the concentration of 10 μM upon addition of ct-DNA (0 μM-20 μM) in phosphate buffer (10 mM, pH 7.4).

Figure 4. Fluorescence spectral changes of compounds **7**, **8, 11**, **12**, **14** and **17** (λ_{ex} = 300 nm) at the concentration of 10 μM upon addition of ct-DNA (0 μM - 20 μM) in phosphate buffer (10 mM, pH 7.4).

Figure 5. Emission spectral changes of BSA at concentration of 10 μM upon addition of compounds **7**, **8, 11, 12, 14** and **17** (0 μM-30 μM) in phosphate buffer (10 mM, pH 7.4).

Table 1. Overview of the preliminary anticancer assay at single dose concentration of 10 μM

Table 2. Compounds **8**, **12**, **14**, **17** and roscovitine having median growth inhibitory (GI_{50}, μM), total growth inhibitory (TGI, μM) and median lethal concentrations (LC_{50}, μM) of *in vitro* subpanel tumor cell lines.

Scheme 1. Synthetic route for the preparation of target compounds **7-18**.

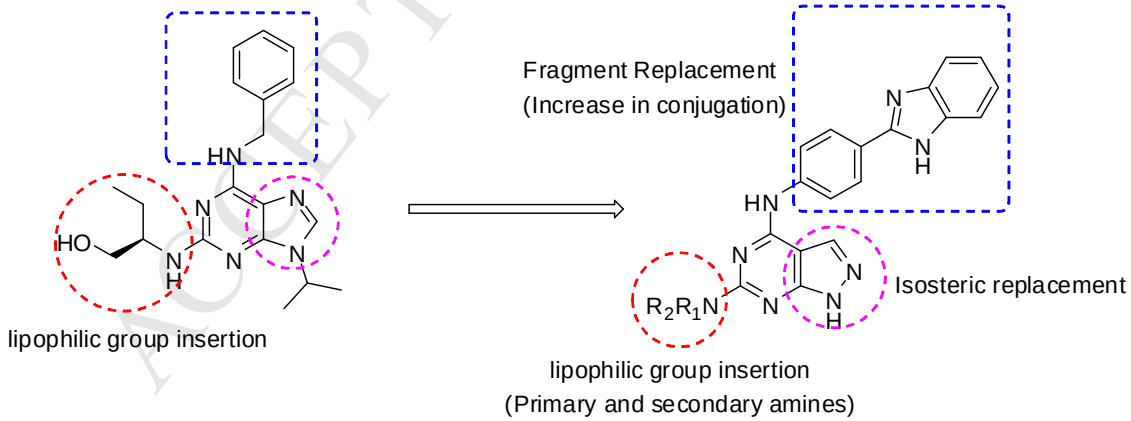

Figure 1. Rational design of the target compounds

A

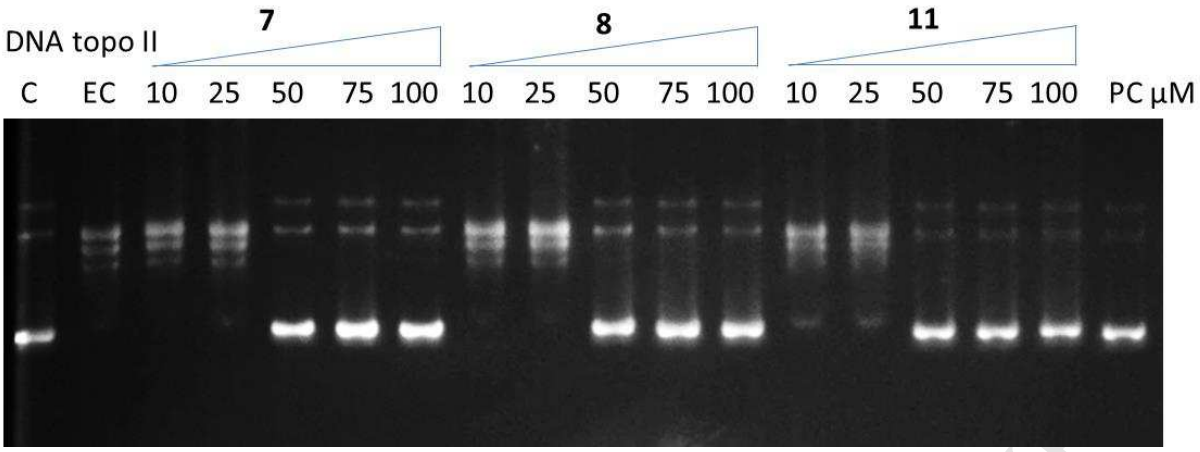

B

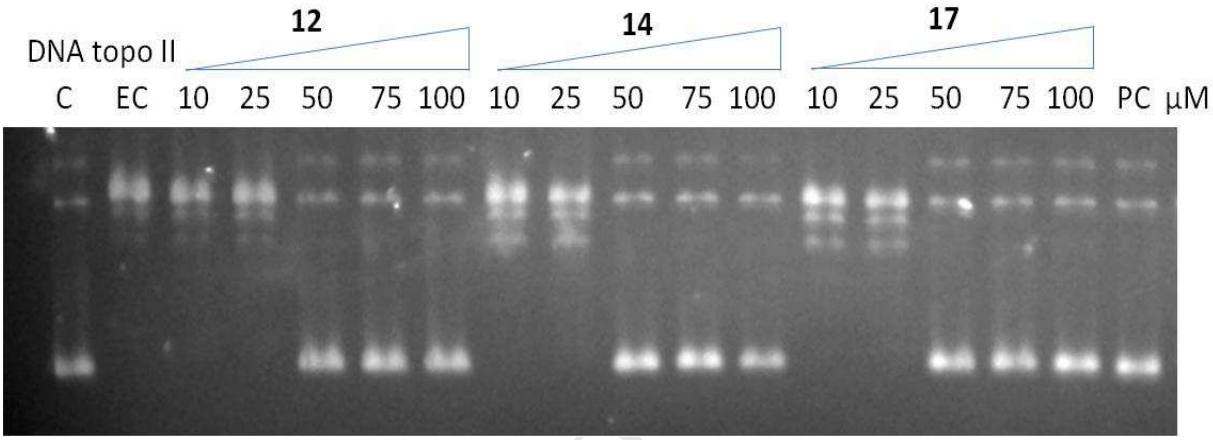

Figure 2. Inhibition of relaxation activity of Topo IIα in the presence of compounds **7, 8**, **11, 12, 14** and **17**. Ethidium bromide stained agarose gel showing: lane 1, pHOT1 plasmid DNA (C); lane 2, relaxation of plasmid DNA by Topo IIα (EC); lanes 3–7 for compound **7** (**A**), lanes 8-12 for compound **8** (**A**) and lanes 13-17 for compound **11** (**A**); lanes 3–7 for compound **12** (**B**), lanes 8-12 for compound **14** (**B**) and lanes 13-17 for compound **17** (**B**) inhibition of relaxation of plasmid DNA by Topo IIα in the presence of 10, 25, 50, 75 and 100 μM of compounds, respectively. Lane 18 indicated the etoposide at 25 μM as positive control (PC).

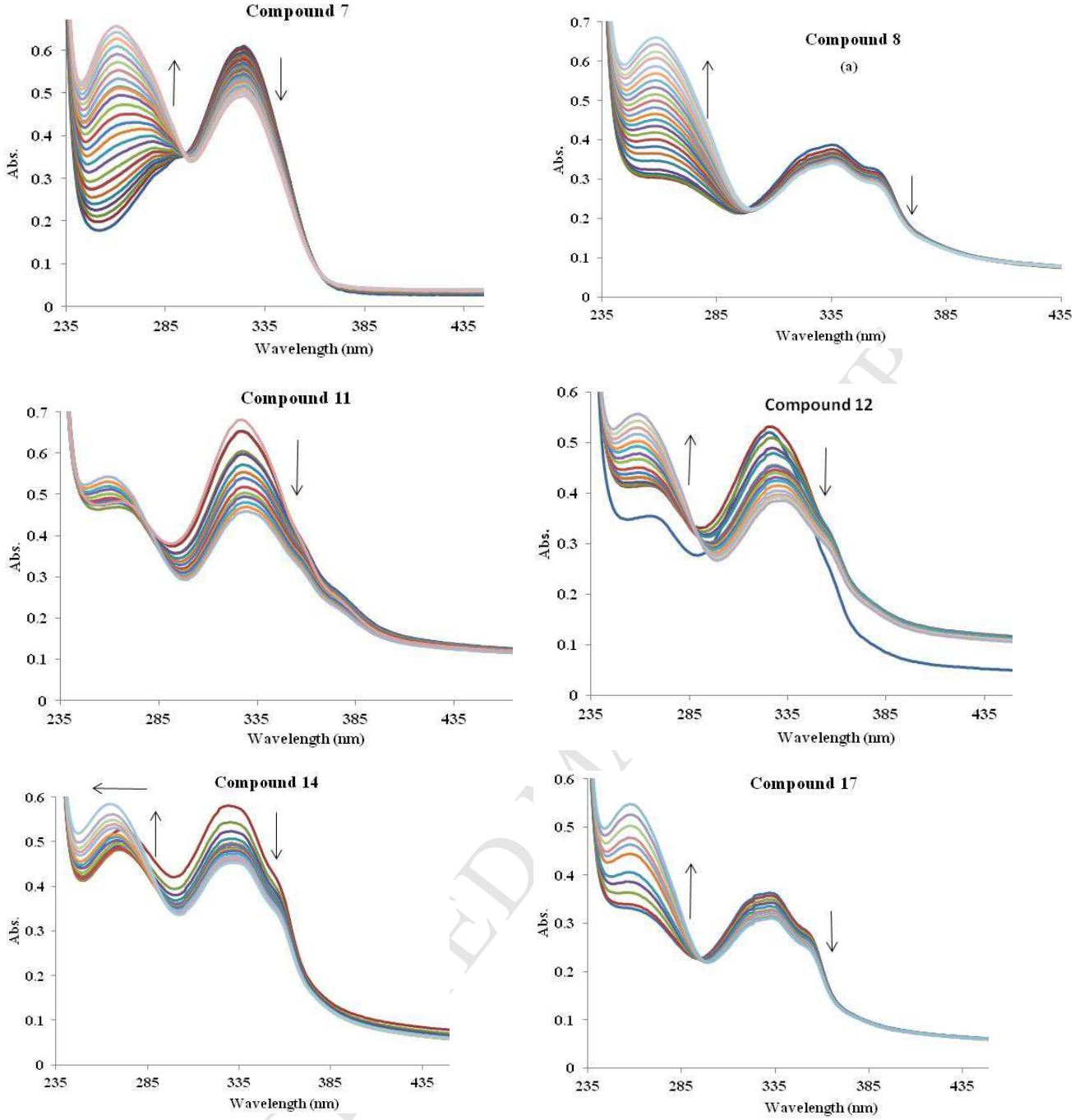

Figure 3. UV-vis spectral changes of compounds **7, 8, 11, 12, 14** and **17** at concentration of 10 μM upon addition of ct-DNA (0 μM-20 μM) in phosphate buffer (10 mM, pH 7.4).

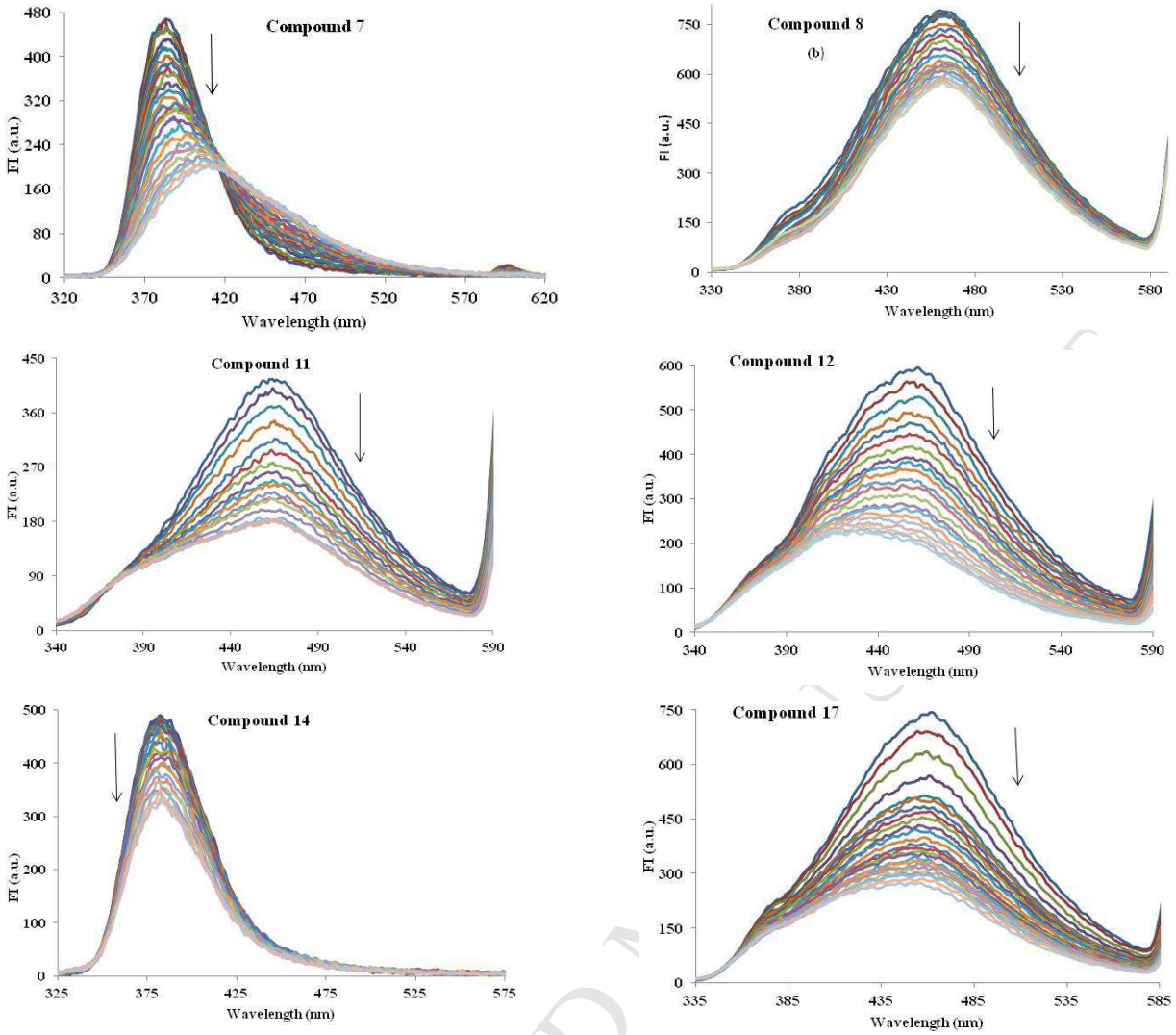

Figure 4. Fluorescence spectral changes of compounds **7**, **8, 11**, **12**, **14** and **17** (λ_{ex} = 300 nm) at the concentration of 10 μM upon addition of ct-DNA (0 μM - 20 μM) in phosphate buffer (10 mM, pH 7.4).

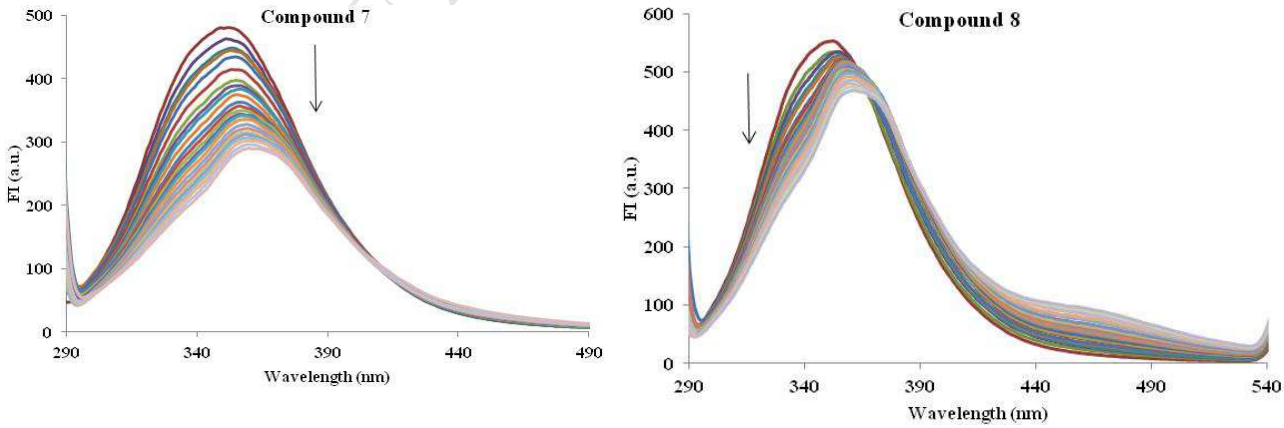

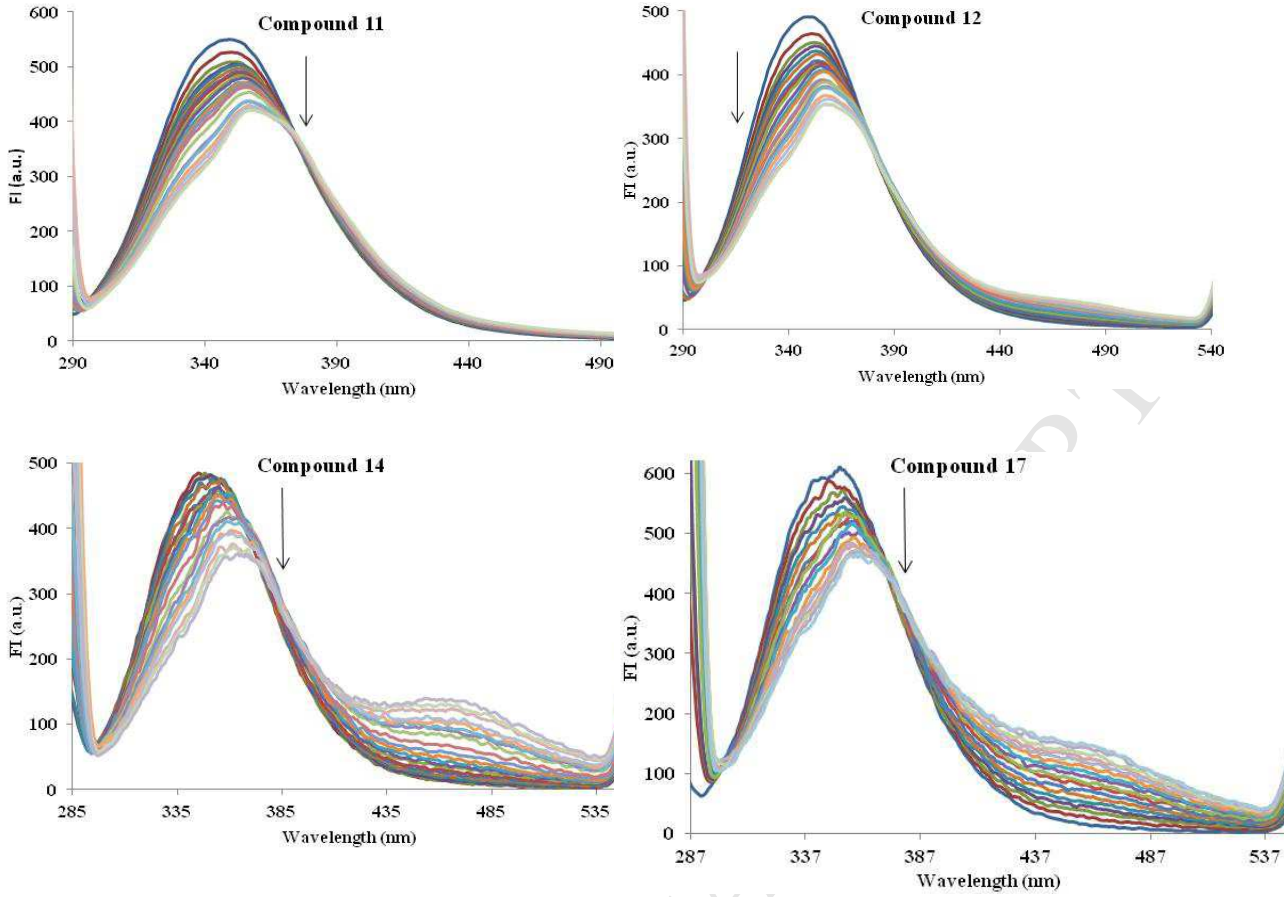

Figure 5. Emission spectral changes of BSA at concentration of 10 μM upon addition of compounds **7**, **8, 11, 12, 14** and **17** (0 μM-30 μM) in phosphate buffer (10 mM, pH 7.4).

Table 1. Overview of the preliminary anticancer assay at single dose concentration of 10 μM

60 cell lines assay in single dose (10 μM)						
Compound No.	Mean Growth %	Range of growth	The most sensitive cell line	Positive cytostatic effect[a]	Positive cytotoxic effect[b]	No. of sensitive cell lines
7	82.24	50.10 to104.00	CCRF-CEM (Leukaemia)	1/54	0/54	1/54
8	-32.52	-92.36 to 98.93	786.0 (renal cancer)	8/55	43/55	51/55
11	61.83	-55.40 to 124.82	U251 (CNS cancer)	11/54	6/54	17/54
12	-77.92	-99.72 to 106.08	U251 (CNS cancer)	1/54	53/54	54/54
14	-8.30	-96.36 to 41.08	SK-MEL-5 (Melanoma)	28/59	31/59	59/59
17	57.44	-64.57 to 107.39	LOX-IMVI (Melanoma)	11/55	6/55	17/55

[a] The ratio between number of cell lines with percent growth from 0-50 and total number of cell lines. [b] The ratio between number of cell lines with percent growth of <0 and total number of cell lines.

Table 2. Compounds **8**, **12**, **14**, **17** and roscovitine having median growth inhibitory (GI_{50}, μM), total growth inhibitory (TGI, μM) and median lethal concentrations (LC_{50}, μM) of *in vitro* subpanel tumor cell lines.

Compounds	Activity	I	II	III	IV	V	VI	VII	VIII	IX	MG-MID[a]
8	GI_{50}	2.38	1.08	2.32	0.86	0.67	1.10	1.22	1.37	0.73	1.30
	TGI	6.70	3.17	5.88	2.01	1.53	2.73	2.67	3.14	2.08	3.32
	LC_{50}	31.8	11.5	2.23	4.17	4.32	6.85	7.04	20.6	6.35	10.5
12	GI_{50}	0.44	1.57	0.72	1.47	1.81	1.84	1.76	1.49	1.80	1.43
	TGI	1.22	3.23	2.12	3.26	3.41	3.59	3.26	2.96	3.83	2.99
	LC_{50}	[b]	6.26	5.71	5.72	5.83	6.09	5.85	5.97	7.02	6.06
14	GI_{50}	2.67	2.54	2.00	2.96	1.85	2.52	2.30	2.56	2.04	2.38
	TGI	6.43	8.99	5.12	16.7	4.29	7.83	6.16	9.43	5.85	7.87
	LC_{50}	[b]	55.3	34.7	28.1	19.3	41.8	31.2	41.8	46.3	37.3
17	GI_{50}	2.62	2.11	1.78	2.06	2.80	2.49	1.84	1.95	1.99	2.18
	TGI	6.33	5.37	3.83	5.08	3.74	6.77	7.35	4.14	4.80	5.27
	LC_{50}	[b]	32.5	6.80	20.4	6.92	28.9	18.2	9.22	19.0	17.7
Roscovitine	GI_{50}	37.5	23.6	24.8	24.7	14.8	29.3	24.9	17.9	22.7	24.5
	TGI	[b]	84.8	84.9	82.2	57.6	93.8	97.0	81.5	73.0	81.8
	LC_{50}	[b]	[b]	[b]	[b]	97.1	[b]	[b]	[b]	94.9	96.0

I, leukaemia; II, non-small cell lung cancer; III, colon cancer; IV, CNS cancer; V, melanoma; VI, ovarian cancer; VII, renal cancer; VIII, prostate cancer; IX, breast cancer. [a] Full panel mean-graph midpoint (μM). [b] Compounds showed values >100 μM.

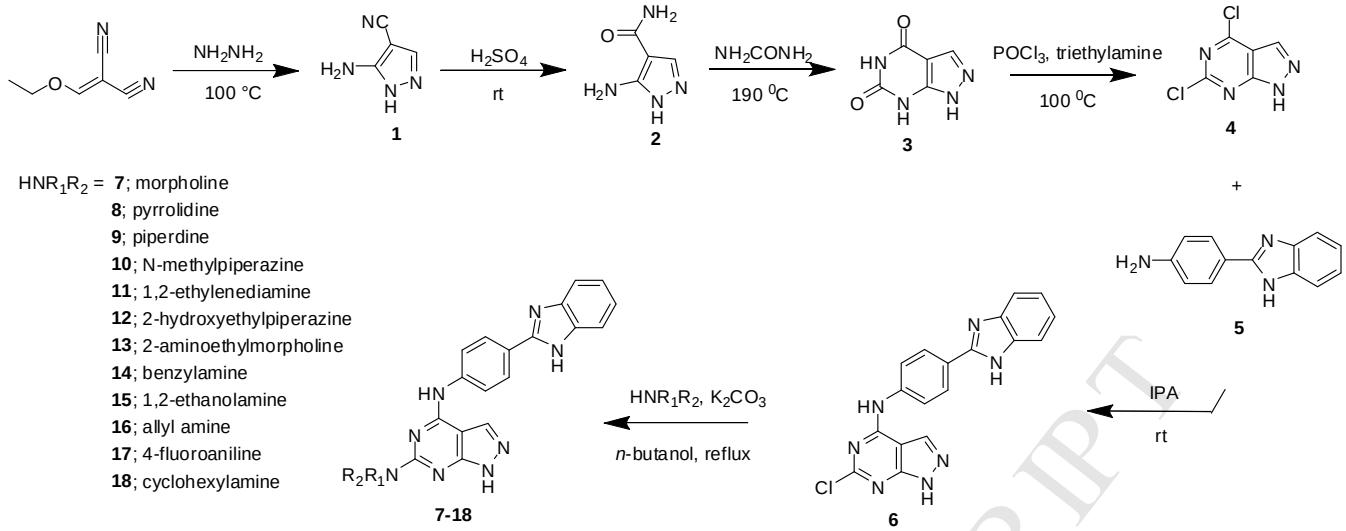

Scheme 1. Synthetic route for the preparation of target compounds **7**-**18**.

Highlights

- A Series of pyrazolo[3,4-*d*]pyrimidine-benzimidazole conjugate has been synthesized.
- Compounds were evaluated *in vitro* for 60 human cancer cell lines.
- Four compounds showed excellent antiproliferative activities.
- Calf thymus-DNA interactions with compounds have been studied.
- Compounds have also been investigated for bovine serum albumin-binding activity.